

**A synergistic effect between 3' terminal noncoding and adjacent coding regions of influenza A virus HA segment on template preference**

Yue Xiao<sup>1,2#</sup>, Wenyu Zhang<sup>#</sup>, Minglei Pan<sup>#</sup>, David L.V. Bauer<sup>2#</sup>, Mengmeng Cao<sup>1</sup>, Yuhai Bi<sup>3</sup>, Ervin Fodor<sup>2\*</sup>, Tao Deng<sup>1,3\*</sup>

<sup>1</sup>NHC Key Laboratory of Systems Biology of Pathogens, Institute of Pathogen Biology, Chinese Academy of Medical Sciences and Peking Union Medical College, Beijing 100176, China

<sup>2</sup>Sir William Dunn School of Pathology, University of Oxford, South Parks Road, Oxford OX1 3RE, United Kingdom

<sup>3</sup>CAS Key Laboratory of Pathogenic Microbiology and Immunology, Institute of Microbiology, Chinese Academy of Sciences, Beijing 100101, China

Short title: Role of RNA sequence in influenza virus replication

<sup>#</sup> These authors contribute equally

\*Correspondence to:

Tao Deng, dengt@im.ac.cn;

Ervin Fodor, ervin.fodor@path.ox.ac.uk

32

33 **ABSTRACT**

34 The influenza A virus genome is comprised of eight single-stranded negative-  
35 sense viral RNA (vRNA) segments. Each of the eight vRNA segments  
36 contains segment-specific nonconserved noncoding regions (NCRs) of similar  
37 sequence and length in different influenza A virus strains. However, in the  
38 subtype-determinant segments, encoding haemagglutinin (HA) and  
39 neuraminidase (NA), the segment-specific noncoding regions are subtype-  
40 specific, varying significantly in sequence and length at both the 3' and 5'  
41 termini among different subtypes. The significance of these subtype-specific  
42 noncoding regions (ssNCR) in the influenza virus replication cycle is not fully  
43 understood. In this study, we show that truncations of the 3'-end H1-subtype-  
44 specific noncoding region (H1-ssNCR) resulted in recombinant viruses with  
45 decreased HA vRNA replication and attenuated growth phenotype, although  
46 the vRNA replication was not affected in single-template RNP reconstitution  
47 assays. The attenuated viruses were unstable and point mutations at  
48 nucleotide position 76 or 56 in the adjacent coding region of HA vRNA were  
49 found after serial passage. The mutations restored the HA vRNA replication  
50 and reversed the attenuated virus growth phenotype. We propose that the  
51 terminal noncoding and adjacent coding regions act synergistically to ensure  
52 optimal levels of HA vRNA replication in a multi-segment environment. These  
53 results, provide novel insights into the role of the 3'-end nonconserved  
54 noncoding regions and adjacent coding regions in the replication of vRNA  
55 segments.

56

57 **IMPORTANCE**

58 While most influenza A virus vRNA segments contain segment-specific  
59 nonconserved noncoding regions of similar length and sequence, these  
60 regions vary considerably both in length and sequence in the segments  
61 encoding HA and NA, the two major antigenic determinants of influenza A  
62 viruses. In this study, we investigated the function of the 3'-end H1-ssNCR  
63 and observed a synergistic effect between the 3'-end H1-ssNCR nucleotides  
64 and adjacent coding nucleotide(s) of HA segment on template preference in a  
65 multi-segment environment. The results unravel an additional level of  
66 complexity in the regulation of RNA replication in multiple-segmented  
67 negative-strand RNA viruses.

68 **KEYWORDS**

69 Influenza A virus, HA segment-specific noncoding nucleotides, transcription,  
70 replication, viral RNA promoter, genome packaging

71

72

## 73 INTRODUCTION

74 Influenza A viruses are a major health threat that cause seasonal epidemics  
75 as well as occasional global pandemics (1). The genome of influenza A  
76 viruses consists of eight single-stranded negative-sense viral RNA (vRNA)  
77 segments which associate with the viral polymerase and nucleoprotein (NP)  
78 to form viral ribonucleoprotein (vRNP) complexes (2). The viral polymerase  
79 consists of three subunits, polymerase basic 1 (PB1), polymerase basic 2  
80 (PB2), polymerase acidic (PA) proteins and carries out transcription and  
81 replication of the vRNA in the nucleus of infected cells. Transcription of the  
82 negative-sense vRNA genome produces positive-sense viral mRNAs with a 5'  
83 terminal N7-methyl guanosine (m<sup>7</sup>G) cap and 3' poly(A) tail (3, 4) During  
84 transcription, the viral polymerase makes an essential interaction with the C-  
85 terminal domain (CTD) of the large subunit of cellular RNA polymerase II (5).  
86 Replication of the negative-sense vRNA genome is a two-step process that  
87 requires polymerase dimerization (6-10). In the first step, the viral polymerase  
88 copies the vRNA template into a positive-sense complementary RNA (cRNA)  
89 replicative intermediate which in the second step serves as template for the  
90 polymerase to synthesize vRNA. Both cRNA and vRNA assemble into RNP  
91 complexes with newly synthesized polymerase and NP (11). Progeny vRNPs  
92 are exported from the cell nucleus and are selectively packaged into progeny  
93 virions which are released from the infected cells by budding (12).

94 Each influenza A virus vRNA segment encodes one or two major open  
95 reading frames in the negative sense which are flanked by 3' and 5' non-  
96 coding terminal sequences. The first 12 and 13 nucleotides at the 3' and 5'  
97 ends, respectively, are highly conserved among different vRNA segments and  
98 form a promoter structure which is bound by the viral polymerase (13). The  
99 conserved terminal promoter sequences and coding region are separated by  
100 nonconserved noncoding regions (NCRs), which are variable in length and  
101 nucleotide composition in different vRNA segments but in most instances are  
102 highly conserved in the same vRNA segment of different influenza virus  
103 strains (14). In the subtype-determinant segments, encoding haemagglutinin  
104 (HA) and neuraminidase (NA), the segment-specific NCRs are also subtype-  
105 specific, varying significantly in length and sequence at both the 3' and 5'  
106 ends among the different subtypes (15).

107 The NCRs are known to play multiple roles in the replication cycle of influenza  
108 A viruses. These include regulatory roles in transcription and replication of  
109 vRNA segments as well as roles in determining splicing and translation  
110 efficiencies (16-22). NCRs and the adjacent coding regions have also been  
111 proposed to contain signals that are required for selective packaging of the  
112 eight vRNA segments into progeny virions (23-37).

In this study, we aimed to characterise the role of the 3'-terminal NCR in the HA vRNA of influenza A virus. These regions differ in length (ranging between 5 to 32 nucleotides) as well as sequence between different influenza A subtypes suggesting a subtype-specific role (15). Here we focus on the 3'-terminal NCR of the H1 subtype vRNA that is characterised by a 20 nucleotide-long U-rich sequence. We demonstrate that HA vRNA templates with truncations in 3'-end H1-subtype-specific noncoding region (3'-end H1-ssNCR) are replicated less efficiently compared to the wildtype HA vRNA template, leading to viral attenuation. However, point mutations (G76A or C56U/A; numbering starting from the 3'-end) in the coding region of the HA vRNA segment reverses the deficiency in vRNA replication and restores virus replication. These results highlight the importance of sequences beyond the conserved promoter structure for vRNA template utilization.

## RESULTS

### **The 3'-end H1-ssNCR is not required for transcription and replication in a single template RNP reconstitution assays.**

To assess the importance of the 3'-end H1-ssNCR for the replication of influenza A virus, we first generated six pHW2000 plasmids to express the HA vRNA segment of influenza A/WSN/33 (H1N1) virus with truncations in the 3'-end H1-ssNCR. Specifically, we progressively truncated the 3'-end H1-ssNCR by deleting three nucleotides at a time upstream of the HA start codon, producing mutants 3L1, 3L2, 3L3, 3L4, 3L5, and 3L6 with 3, 6, 9, 12, 15, and 18 nt deletions, respectively (Fig. 1A).

To characterise the effect of 3'-end H1-ssNCR truncations on RNA synthesis, vRNPs were reconstituted by coexpression of the three polymerase subunits, NP and wildtype or 3'-end H1-ssNCR truncated HA vRNA in human HEK-293T cells and the steady-state levels of positive- and negative-sense RNAs were analysed by primer extension. The catalytically inactive polymerase (PB1a) was used as negative control (38). All 3'-end H1-ssNCR truncated HA vRNAs were transcribed and replicated by the viral polymerase to levels similar to that of the wildtype HA vRNA (Fig. 1B). These results suggest that the conserved 12 nucleotides and the two adjacent HA segment-specific CC nucleotides at the 3'-end of HA vRNA (as present in the 3L6 mutant) are sufficient for viral polymerase to efficiently replicate and transcribe the vRNA in a single template RNP reconstitution system.

To address whether this result is specific to influenza A/WSN/33 or could be generalised to other influenza A virus strains, we introduced the same 3'-end H1-ssNCR truncations into the HA segment of the pandemic A/California/04/2009 (H1N1) virus (CA04) and examined the effect of the

truncations on RNA synthesis in the context of the CA04 vRNP reconstitution system. We obtained similar results as with the WSN virus (Fig. 1C). Together, these results show that the 3'-end H1-ssNCR is not required for transcription and replication in a single-template RNP reconstitution assay.

### **Truncations of the 3'-end H1-ssNCR lead to virus attenuation.**

Next, we used reverse genetics to generate WSN and CA04 viruses with 3'-end H1-ssNCR truncations and titres of the rescued viruses (P0) were examined. In the context of WSN viruses, the 3L1 and 3L2 viruses showed similar titres compared to the wildtype virus, while the 3L3 virus showed about a 10-fold reduction. The 3L4 and 3L5 viruses were severely attenuated showing more than 3 log reduction. No plaques were detected for the 3L6 virus (Fig. 2A).

In the case of CA04 viruses (P0), all truncation mutants (3L1-3L6) could be rescued and we measured the virus replication efficiency by TCID<sub>50</sub>. As shown in Fig. 2B, we observed similar titres for the rescued WT and 3L1-4 mutant viruses, but the titres of 3L5 and 3L6 mutant viruses were significantly lower than WT. Taken together, these results suggest that 3'-end H1-ssNCR truncations lead to virus attenuation and reduction in virus production although the extents vary between different truncations and different viruses.

### **Attenuated P0 viruses show improved growth upon virus passage.**

To further characterise these 3'-end H1-ssNCR truncated mutant viruses, the rescued WSN virus (P0) was then passaged in MDCK cells. Interestingly, the growth curves of all passaged WSN viruses (P2) in MDCK cells, including the 3L4 and 3L5 mutants, reached maximal viral titres between  $1 \times 10^7$  to  $1 \times 10^8$  pfu/ml, similar to wildtype (Fig. 2C). To address the molecular basis of the improved growth, we sequenced the 3' terminus of HA vRNA of WSN viruses (P2). We found that 3L3, 3L4 and 3L5 mutants were unstable and contained mutations in addition to the truncations introduced. In the 3L3 mutant we observed a duplication of six nucleotides, resulting in the insertion of UAUUUU (ATAAAA in positive sense) upstream of the HA start codon, extending the 3'-end H1-ssNCR to a length identical to that in 3L1. In mutant viruses 3L4 and 3L5, a point mutation G76A (C76T in positive sense) was found in the HA open reading frame, which changes the 15th HA amino acid from threonine to isoleucine. We also passaged these mutant WSN viruses in A549 cells and sequenced the virus at P2. We found exactly the same mutations as described above for 3L3, 3L4 and 3L5. Moreover, we repeatedly found an independent C56U mutation in the HA open reading frame of mutant virus 3L5 (Fig. 2E). For the highly attenuated 3L5 and 3L6 CA04 mutant viruses we did not observe any improved CPE after 10 passages in MDCK cells. We then passaged these viruses in embryonated chicken eggs and analysed virus titres by TCID<sub>50</sub>. The CA04 3L6 mutant showed significantly

194 higher virus titres than 3L5 at P6 (Fig. 2D). We sequenced the CA04 3L6 (P6)  
195 virus and found a synonymous mutation C56A (CUG-CUU) at exactly the  
196 same position as we found in WSN 3L5 virus passaged in A549 cells (Fig.  
197 2F). Together, these results show that the 3L3, 3L4 and 3L5 mutant WSN  
198 viruses and the 3L6 CA04 virus with 3'-end H1-ssNCR truncations are  
199 unstable and upon passage they can accumulate mutations at specific  
200 positions in the adjacent HA coding region which might improve their growth.

201 **The G76A and C56U mutations are responsible for the improved growth**  
202 **of the attenuated viruses.**

203 In order to assess the effect of the G76A mutation on WSN virus growth we  
204 generated recombinant viruses WT-G76A, 3L4-G76A and 3L5-G76A using  
205 reverse genetics and titres of the rescued viruses (P0) were examined by  
206 plaque assay. In contrast to the significant attenuation (3 log reduction)  
207 observed for the original 3L4 and 3L5 mutants, the 3L4-G76A and the 3L5-  
208 G76A mutants showed similar titres as the wildtype virus (Fig. 3A). We  
209 sequenced the 3' terminus of the HA vRNA of the 3L4, 3L4-G76A, 3L5 and  
210 3L5-G76A viruses and found that in the 3L4 and 3L5 viruses, both G and A (C  
211 and T in positive sense) were present at position 76, indicating that these  
212 viruses are unstable and obtain the G76A mutation very quickly. In contrast,  
213 no mutation was observed at position 76 or at any other position in the  
214 sequenced part of the 3' terminus of the HA vRNA (position 1 to 151) of the  
215 3L4-G76A and 3L5-G76A viruses (Fig. 3B). To address if the C56U mutation  
216 has the same effect as the G76A mutation, we plaque purified both 3L5-G76A  
217 and 3L5-C56U mutant viruses and examined virus growth by plaque assay.  
218 The 3L5-C56U mutant showed similar titre as the 3L5-G76A mutant and  
219 wildtype virus (Fig. 3C). Together these results show that the G76A and C56U  
220 mutations in the open reading frame of the HA vRNA stabilise the 3L4 and  
221 3L5 viruses with 3'-end H1-ssNCR truncations and reverse the attenuation in  
222 virus replication.

223 **The 3'-end H1-ssNCR truncated mutant viruses show decreased HA**  
224 **vRNA levels in virions and in cells.**

225 To address which step in the virus life cycle is affected by the truncations in  
226 the 3'-end H1-ssNCR and to elucidate how the G76A mutation improves viral  
227 growth, we analysed HA vRNA levels in the rescued WSN virus (P0) as well  
228 as in the transfected cells used for the generation of P0 stock of virus using  
229 RT-qPCR. Compared to the levels of NA vRNA, the 3'-end H1-ssNCR  
230 truncated mutant WSN viruses 3L2, 3L3, 3L4 and 3L5 showed decreased  
231 levels of HA vRNA in both the harvested virions and the transfected cells.  
232 However, the G76A mutation in the 3L4-G76A and 3L5-G76A viruses  
233 significantly increased the HA vRNA levels in both virions and cells (Fig. 4A).

234 To investigate the reduction in HA vRNA levels further, the rescued viruses

(P0) were passaged in MDCK cells (P1). At 24 h post-infection RNA was isolated from the passaged viruses and the infected cells, followed by the analysis of HA vRNA by RT-qPCR. In general, the results were consistent with the results observed before passage, showing that 3'-end H1-ssNCR truncations lead to decreased HA vRNA levels in both virions and cells while the G76A mutation increased HA vRNA levels (Fig. 4B). Together, these results show that truncations in the 3'-end H1-ssNCR lead to deficiency in RNA replication, resulting in decreased HA vRNA levels in cells and thus in virions. The G76A mutation increases HA vRNA levels in cells and thus in virions, promoting the improved replication of the 3'-end H1-ssNCR truncated mutant viruses.

**The 3'-end H1-ssNCR truncated mutant templates are replicated less efficiently than the wildtype HA template in multiple-template vRNP reconstitution assays.**

The findings above demonstrate that truncations in the 3'-end H1-ssNCR do not significantly affect RNA synthesis in a single-template vRNP reconstitution assay (Fig. 1B) but result in decreased HA vRNA levels in virions and in cells during viral rescue and virus passage (Fig.4). It has been proposed that the gene segments of influenza A viruses could compete for available viral polymerase (39). To address the effect of truncations in 3'-end H1-ssNCR, seven pHW2000 plasmids (PB2, PB1, PA, NP, HA (wildtype or mutant), NA, NS) were cotransfected into human HEK-293T cells and the accumulation of positive- and negative-sense RNAs was analysed by primer extension. The pHW2000-M plasmid was excluded to avoid the formation of virus particles. Mutant HA vRNA templates with 3'-end H1-ssNCR truncations showed reduced steady-state levels of mRNA, cRNA and vRNA compared to the wildtype HA segment. However, the 3L4-G76A and 3L5-G76A mutant HA vRNA templates with the additional G76A mutation showed increased RNA levels compared to those without the G76A mutation (Fig. 5A, top). The steady-state levels of mRNA, cRNA and vRNA derived from the NA segment were not affected (Fig. 5A, bottom). We conducted the same experiment described above for the CA04 3'-end H1-ssNCR truncation mutants and obtained very similar results (Fig. 5B).

The results above indicate that the HA vRNA templates with 3'-end H1-ssNCR truncations are transcribed and replicated less efficiently than the wildtype HA vRNA template. To address this further, we carried out a vRNP reconstitution assay in which we coexpressed wildtype HA vRNA and a 3'-end H1-ssNCR truncated HA vRNA, together with plasmids expressing polymerase and nucleoprotein. We used a transcription-deficient polymerase (PA-D108A) (40) to avoid the generation of mRNA which produces a signal that overlaps with cRNA hampering the quantitation of primer extension analyses. In comparison to the steady-state level of the wildtype HA vRNA

template, the 3L2 to 3L6 3'-end H1-ssNCR truncated mutant vRNA templates produced significantly reduced levels of cRNA. However, the 3L4-G76A and 3L5-G76A mutant templates with the additional G76A mutation produced significantly increased levels of cRNA compared to 3L4 and 3L5 without the G76A mutation and were not significantly different compared to cRNA levels produced by the wildtype HA vRNA template (Fig. 6A). We also observed similar effects when the C56U mutation was introduced into the 3L4 and 3L5 mutants (Fig. 6B). Together these results show that the 3L2 to 3L6 3'-end H1-ssNCR truncated mutants have a disadvantage compared to the wildtype HA segment in RNA synthesis. However, the introduction of the G76A or the C56U mutation in the 3L4 and 3L5 mutants eliminates this disadvantage and restores the deficiencies in RNA synthesis.

## DISCUSSION

In this study, we aimed to characterise the role of the 3'-end H1-ssNCR in the HA vRNA of influenza A viruses. We found that 3'-end H1-ssNCR truncated mutant templates could be transcribed and replicated as efficiently as the wildtype template in single-template RNP reconstitution assays. However, recombinant viruses (WSN and CA04) with truncations in the 3'-end H1-ssNCR showed decreased HA vRNA levels both in virions and infected cells and those with the longest deletions were severely attenuated. This was the result of reduced replication of the mutant HA vRNAs in the presence of the other seven vRNA segments in both transfected and infected cells. Interestingly, we found that a point mutation at specific position located in the adjacent HA coding region of the attenuated viruses could restore the HA vRNA levels and virus growth. We propose that although not essential, the 3'-end H1-ssNCR as well as the adjacent coding region play a role in determining how efficiently the viral polymerase transcribes and replicates a template in the presence of the other seven vRNA templates during influenza A virus replication.

It has been reported that mutations introduced into the 3'-end NCR of a segment led to the reduction of this segment both in infected cells and in virions (16, 17), while other studies using vRNP reconstitution assays found no evidence for a significant role of 3'-end NCR in regulating viral RNA synthesis (15, 18). We show here that the conserved 12 nucleotides and the two adjacent HA segment-specific CC nucleotides at the 3'-end of HA vRNA (as present in the 3L6 mutant) are sufficient for the viral polymerase to efficiently replicate and transcribe the vRNA in a single template vRNP reconstitution system. However, in a multi-segment environment, such as during reverse genetics and viral infection, we observed a reduced replication of the 3'-end H1-ssNCR mutants indicating that 3'-end NCRs influence replication and transcription and contribute to the fine-tuning of these



processes. This is consistent with a previous report in which it was proposed that influenza virus genome segments could compete for available polymerase, especially at early stage of infection. The ability of a segment to compete is dependent on its length and sequences both in the coding region and untranslated regions although the mechanisms involved remain unknown (38). Our study, for the first time, reveals very distinct synthesis capacities of the same 3'-end NCR mutant templates in single-segment and multi-segment environments and as such may help resolving the inconsistent conclusions on the regulatory role of the nonconserved NCR reported in the literature. It would be interesting to test whether 5'-end H1-ssNCR mutants have similar effects. Our data could be particularly relevant to the vRNA segments encoding HA and NA which are known to act antagonistically and their activities have to be balanced during viral infection (41-45). The subtype-specific variation in sequence and length of NCRs of HA and NA vRNA could be a mechanism by which the levels of HA and NA are fine-tuned in different influenza A virus subtypes.

Upon viral passage we have identified an insertion in the 3'-end H1 ssNCR and a point mutation in the coding region of HA vRNA which improved viral growth. It remains unclear how a single nucleotide mutation more than 20-40 nucleotides downstream of the mutated 3'-end H1 ssNCR restores vRNA replication. A recent study investigating the global high-resolution structure of the influenza A virus genome showed that vRNA in the context of vRNP is capable of accommodating secondary RNA structures with extensive base pairing (46). Le Sage et al recently reported that vRNA-vRNA interactions in the context of vRNPs are highly flexible and redundant (47). We speculate that truncations in the segment-specific noncoding region could inhibit the formation of a beneficial secondary structure or promote the formation of an inhibitory secondary structure and the single nucleotide mutation could revert this. Alternatively, considering that different reversion mutations were obtained in different hosts (G76A for WSN in MDCK cells, either G76A or C56U for WSN in A549 cells, and C56A for CA04 in eggs), we speculate that the synergistic effect between 3' terminal noncoding and adjacent coding regions of the H1 vRNA could also be mediated by a host factor. However, the underlying mechanisms that lead to the reversal of viral attenuation as a result of these single nucleotide mutations remain unknown and need further studies to clarify. It should also be noted that the effect of 3'-end H1 ssNCR truncations on vRNA replication could be due to defects in the second step of replication, i.e. the replication of cRNA into vRNA, with the mutations affecting the 5'-end of the HA cRNA. In multi-segment vRNP reconstitution assays mRNA levels were also affected (Fig. 5). It remains unclear whether this reduction in mRNA is a result of reduced vRNA template levels or the truncations directly affect transcription as well.

It has been proposed that the 3' and 5' NCRs, together with its adjacent

terminal coding regions of each segment serve as segment-specific packaging signals in the selective genome-packaging model (29). However, replication of the mutant HA templates used in previous studies was mainly examined in single-template vRNP reconstitution assays. It is unclear whether the reductions in HA vRNA in virions were entirely due to reduced packaging or reduced replication in a multi-segment environment. In our study, we cannot exclude the possibility that the packaging efficiency of HA vRNA is also affected in the 3'-end H1-ssNCR truncated mutant viruses. We speculate that the nucleotides in the ssNCRs of HA segment might function as cis-acting signals in both vRNA replication and HA vRNA packaging. Furthermore, one could argue that defective particles (DI) could be generated upon reduction of HA vRNA due to a packaging defect (35). However, considering that the segment with the single nucleotide mutation quickly outcompeted the truncated segment and the HA vRNA levels in virions recovered to wildtype levels after two virus passages, it is unlikely that a lot of DI particles would have been generated which would have interfered with virus growth in passage one and two.

In summary, we demonstrate that 3'-end H1-ssNCR truncations lead to decreased HA-specific RNA synthesis, resulting in virus attenuation. Point mutations found in the adjacent coding region reverse the defect in vRNA replication and restores virus growth. These findings unravel the importance of the NCR and the adjacent coding region in regulating the replication and transcription of vRNA segments during influenza A virus replication.

## MATERIALS AND METHODS

**Cells, viruses and plasmids.** Human embryonic kidney 293T (HEK-293T) cells and human lung carcinoma cell line A549 were cultured in Dulbecco modified Eagle medium (DMEM) supplemented with 10% fetal calf serum (FCS). Madin-Darby canine kidney (MDCK) were cultured in minimal essential medium (MEM) supplemented with 10% FCS and 2mM L-glutamine. Cells were maintained at 37°C and 5% CO<sub>2</sub>. Plasmids pcDNA-PB2, pcDNA-PB1, pcDNA-PA, pcDNA-NP, pcDNA-PB1a for the vRNP reconstitution system of influenza A/WSN/33 (H1N1) virus (38, 48) have been described previously. Recombinant influenza A/WSN/33 (H1N1) virus was generated using the pHW2000 eight-plasmid system (49). The pHW2000 eight-plasmid system and the RNP reconstitution system of influenza A/California/04/2009 (H1N1) virus were generated in the same way as those of the WSN virus. Plasmids pHW2000-HA-3L1 to pHW2000-HA-3L6 were generated from pHW2000-HA by PCR amplification of the HA sequences with corresponding primers introducing truncations in the 3'-end H1-ssNCR. The PCR products were then ligated into the BsmBI site of the pHW2000 vector. To construct pHW2000-

mut plasmid to express vRNA but not mRNA, the pHW2000 plasmid was modified by removing the truncated immediate-early promoter of the human cytomegalovirus (CMV). The plasmids pHW2000-mut-HA-3L1 to pHW2000-mut-HA-3L6 were then generated by ligating the PCR products mentioned above into the pHW2000-mut plasmid. The plasmids with G76A or C56U mutation were generated from the corresponding pHW2000-HA or pHW2000-mut-HA plasmids using site-directed PCR mutagenesis.

**Reverse genetics.** Recombinant influenza A/WSN/33 (H1N1) (WSN) virus or influenza A/California/04/2009 (H1N1) (CA04) virus was generated using the pHW2000 eight-plasmid system (49). Approximately  $10^6$  HEK-293T cells were transfected with 0.5  $\mu$ g each of pHW2000-PB2, pHW2000-PB1, pHW2000-PA, pHW2000-HA (wildtype or mutant), pHW2000-NP, pHW2000-NA, pHW2000-M, pHW2000-NS using Lipofectamine 2000 and Opti-MEM according to the manufacturer's instructions. At 24 h post-transfection, DMEM containing 10% FCS was replaced with DMEM containing 0.5% FCS and 100 U/ml Penicillin-Streptomycin (ThermoFisher). The virus supernatant was harvested 48 h after changing medium. For serial passage, A/WSN/33 wildtype and mutant viruses were used to infect MDCK or A549 cells at a multiplicity of infection (MOI) of 0.001. A/California/04/2009 wildtype and mutant viruses were diluted 10 fold with Opti-MEM and serial passaged in 9-day-old embryonated eggs (50). The virus titre was examined by plaque assay (A/WSN/33 virus) or TCID<sub>50</sub> (A/California/04/2009 virus).

**RNA sequencing.** The RNA of virus stock was extracted with TRI LS Reagent (Sigma-Aldrich) and reverse transcribed using the SuperScript III first-strand synthesis system (Invitrogen) with universal influenza A virus reverse transcription (RT) primers (vRNA\_3\_ga GTTCAGACGTGTGCTCTTCCGATCTAGCGAAAGCAGG; vRNA\_3\_aa GTTCAGACGTGTGCTCTTCCGATCTAGCAAAAGCAGG) (the nucleotide corresponding to position 4 at the 3'-end of vRNA which can be either U or C is underlined). The RT products were then amplified by PCR using HA segment-specific primers (Fwd\_5'-GTGCTCTTCCGATCTAGCAAAAGCAGG-3'; Rev\_5'-GATGTTACATTTCCCAATTGTAGTGGGGC-3' (A/WSN/33 virus); Rev\_5'-GGTGTTCACAAATGTAGGACCATGAGCT-3' (A/California/04/2009 virus)), followed by sequencing of the PCR product.

**Virus growth curve.** MDCK cells were infected with either wildtype WSN or recombinant virus at a multiplicity of infection (MOI) of 0.001. At 24, 36, 48, 60, 72 h post-infection (p.i.), the supernatants were collected. The virus titres were determined by plaque assay on MDCK cells.

**vRNP reconstitution assay and primer extension analysis.** For single-template vRNP reconstitution assays, vRNPs were reconstituted by transiently transfecting approximately  $10^6$  HEK-293T cells with 1  $\mu$ g each of pcDNA-PB2,

pcDNA-PB1/ pcDNA-PB1a, pcDNA-PA, pcDNA-NP and pHW2000-mut-HA (wildtype or mutant) using Lipofectamine 2000 and Opti-MEM according to the manufacturer's instructions. For double-template vRNP reconstitution assays with a transcription-deficient but replication-competent polymerase (D108A) (40), approximately  $10^6$  HEK-293T cells were transfected as before with 1  $\mu$ g each of pcDNA-PB2, pcDNA-PB1/ pcDNA-PB1a, pcDNA-PA-D108A, pcDNA-NP and pHW2000-mut-HA (wildtype and mutant). For seven-template vRNP reconstitution assays, pHW2000-PB2, -PB1, -PA, -HA (wildtype or mutant), -NP, -NA and -NS plasmids were transfected into HEK-293T cells. Plasmids pcDNA-PB1a and pPOLI-PB1 encoding polymerase with an active site mutation (D445A/446A) (38) were used as negative control. Cells were harvested 24 h post-transfection. Total RNA was extracted using TRI Reagent (Sigma-Aldrich) and dissolved in 20  $\mu$ l of nuclease-free water. RNA was analysed by primer extension using  $^{32}$ P-labelled primers specific for negative- or positive-sense viral RNAs as well as 5S rRNA. The primers for segment 4 or 6 negative- or positive-sense RNA of A/WSN/33 virus and 5S rRNA have been described previously (51). 5S rRNA was used as internal loading control. In order to improve the separation of primer extension products from segment 4 negative- and positive-sense RNAs of the 3'-end H1-ssNCR truncated WSN mutants, primer 5'-TTCGAGCAGGTTAACAGAATG-3' was used to analyse the positive-sense HA RNAs. For the vRNP reconstitution assays using pcDNA-PA-D108A, primer 5'-GCTACAAATGCATATAACAGGACC-3' or 5'-AGGACCAGTAGTTTTGCC-3' annealing close to the 5' terminus of HA cRNA was used to analyse HA cRNA. For A/California/04/2009 virus, primer 5'-CTTCTAGAAGGTTAACAGAGTGTG-3' was used to detect positive-sense RNA. Primer 5'-ATTGGTACTGGTAGTCTCCC-3' was used to detect negative-sense RNA. In vRNP reconstitution assays using pcDNA-PA-D108A, primer 5'-GCGGTTGCAAATGTATATAGC-3' annealing close to the 5' terminus of HA cRNA was used to analyse HA cRNA. Primer extension products were analysed by 6% or 12% denaturing PAGE with 7 M urea in Tris-borate-EDTA (TBE) buffer and visualized by phosphor-imaging on an FLA-5000 scanner (Fuji). ImageJ was used to analyze the  $^{32}$ P-derived signal (52).

**qPCR analysis of virion RNA and cellular RNA.** Wildtype or recombinant A/WSN/33 viruses and transfected or infected cells were harvested after virus rescue or infection. Virus was treated with 5  $\mu$ l Benzonase (Novagen) at 37°C for 30min to remove nucleic acids outside the virions. Then virion RNA was extracted using TRI LS Reagent (Sigma-Aldrich), followed by DNase treatment (Turbo) and clean-up by using RNA Clean & Concentrator-5 Kit (Zymo Research). Cellular RNA was extracted using TRI Reagent (Sigma-Aldrich), followed by the same DNase treatment and clean-up as above. The virion RNA or cellular RNA was dissolved in 15  $\mu$ l nuclease-free water. Approximately 40 ng virion RNA or cellular RNA was reverse transcribed by

SuperScript III (Invitrogen) with universal influenza A virus reverse transcription (RT) primers as above. The RT product was then diluted 80 fold and used as template for qPCR. 1 µl of diluted RT product was used for a TaqMan probe-based qPCR reaction using Brilliant III Ultra-Fast Probe High ROX QPCR Master Mix (Agilent Technologies). The TaqMan probes and primer sequences are as follows: HA\_Fw 5'-GTTTGGTGTCTTCTACAATGTAGGACC-3'; HA\_Rv 5'-CGAAGACAGACACAACGGGA-3'; HA\_Taq [JOE]5'-CTGGAAGCAGTGAGTCGCA-3'[BHQ2]; NA\_Fw 5'-CTGTGTATAGCCACCCACG-3'; NA\_Rv 5'-GCAACCAAGGCAGCATTACC-3'; NA\_Taq [JOE]5'-TGCTGGGCAGGACTCAACTTCAGT-3'[BHQ1]. The primers named with “\_Taq” are TaqMan probes labelled with fluorophores (JOE) and quenchers (BHQ1, BHQ2). A 40-cycle qPCR was carried out according to the manufacturer's instructions on a StepOnePlus instrument (Applied Biosystems). Two technical replicates were performed for each segment per sample. The relative concentrations of vRNAs were determined on the basis of an analysis of cycle threshold values.

**Statistics.** GraphPad Prism software, version 6, was used for statistical analysis. Two-way analysis of variance (ANOVA) with Dunnett correction was used for two-variable comparisons while One-way analysis of variance (ANOVA) with Dunnett correction was used for one-variable comparisons. *P* values of <0.05 was considered to be significant.

## ACKNOWLEDGMENTS

We thank Hongjie Zhang (Core Facility for Protein Research, Institute of Crystal Structure of Biophysics, Chinese Academy of Sciences) for technical support with autoradiography. We thank Erich Hoffmann for the pHW2000 plasmids.

This work was supported by grants from the National Mega-Project for Infectious Diseases (2018ZX10101001-004); the CAMS Innovation Fund for Medical Sciences (2016-12M-1-014); UK Medical Research Council (MR/R009945/1) and China Scholarship Council (201806210420).

## REFERENCES

1. **Taubenberger JK, Kash JC.** 2010. Influenza virus evolution, host adaptation, and pandemic formation. *Cell Host Microbe* 7:440-51.
2. **Eisfeld AJ, Neumann G, Kawaoka Y.** 2015. At the centre: influenza A virus ribonucleoproteins. *Nat Rev Microbiol* 13:28-41.
3. **Fodor E, Te Velthuis AJW.** 2020. Structure and Function of the

526 Influenza Virus Transcription and Replication Machinery. Cold Spring  
527 Harb Perspect Med 10.

528 4. **Wandzik JM, Kouba T, Cusack S.** 2020. Structure and Function of  
529 Influenza Polymerase. Cold Spring Harb Perspect Med  
530 doi:10.1101/cshperspect.a038372.

531 5. **Walker AP, Fodor E.** 2019. Interplay between Influenza Virus and the  
532 Host RNA Polymerase II Transcriptional Machinery. Trends Microbiol  
533 27:398-407.

534 6. **Jorba N, Coloma R, Ortin J.** 2009. Genetic trans-complementation  
535 establishes a new model for influenza virus RNA transcription and  
536 replication. PLoS Pathog 5:e1000462.

537 7. **Fan H, Walker AP, Carrique L, Keown JR, Serna Martin I, Karia D,  
538 Sharps J, Hengrung N, Pardon E, Steyaert J, Grimes JM, Fodor E.**  
539 2019. Structures of influenza A virus RNA polymerase offer insight into  
540 viral genome replication. Nature 573:287-290.

541 8. **Moeller A, Kirchdoerfer RN, Potter CS, Carragher B, Wilson IA.**  
542 2012. Organization of the influenza virus replication machinery.  
543 Science 338:1631-4.

544 9. **Chang S, Sun D, Liang H, Wang J, Li J, Guo L, Wang X, Guan C,  
545 Boruah BM, Yuan L, Feng F, Yang M, Wang L, Wang Y, Wojdyla J,  
546 Li L, Wang J, Wang M, Cheng G, Wang HW, Liu Y.** 2015. Cryo-EM  
547 structure of influenza virus RNA polymerase complex at 4.3 Å  
548 resolution. Mol Cell 57:925-935.

549 10. **Carrique L, Fan H, Walker AP, Keown JR, Sharps J, Staller E,  
550 Barclay WS, Fodor E, Grimes JM.** 2020. Host ANP32A mediates the  
551 assembly of the influenza virus replicase. Nature 587:638-643.

552 11. **York A, Hengrung N, Vreede FT, Huiskonen JT, Fodor E.** 2013.  
553 Isolation and characterization of the positive-sense replicative  
554 intermediate of a negative-strand RNA virus. Proc Natl Acad Sci U S A  
555 110:E4238-45.

556 12. **Lakdawala SS, Fodor E, Subbarao K.** 2016. Moving On Out:  
557 Transport and Packaging of Influenza Viral RNA into Virions. Annu Rev  
558 Virol 3:411-427.

559 13. **Robertson JS.** 1979. 5' and 3' terminal nucleotide sequences of the  
560 RNA genome segments of influenza virus. Nucleic Acids Res 6:3745-  
561 57.

562 14. **Desselberger U, Racaniello VR, Zazra JJ, Palese P.** 1980. The 3'  
563 and 5'-terminal sequences of influenza A, B and C virus RNA segments  
564 are highly conserved and show partial inverted complementarity. Gene  
565 8:315-28.

566 15. **Zhao L, Peng Y, Zhou K, Cao M, Wang J, Wang X, Jiang T, Deng T.**  
567 2014. New insights into the nonconserved noncoding region of the  
568 subtype-determinant hemagglutinin and neuraminidase segments of  
569 influenza A viruses. J Virol 88:11493-503.

- 570 16. **Zheng H, Palese P, Garcia-Sastre A.** 1996. Nonconserved  
571 nucleotides at the 3' and 5' ends of an influenza A virus RNA play an  
572 important role in viral RNA replication. *Virology* 217:242-51.
- 573 17. **Bergmann M, Muster T.** 1996. Mutations in the nonconserved  
574 noncoding sequences of the influenza A virus segments affect viral  
575 vRNA formation. *Virus Res* 44:23-31.
- 576 18. **Wang J, Peng Y, Zhao L, Cao M, Hung T, Deng T.** 2015. Influenza A  
577 virus utilizes a suboptimal Kozak sequence to fine-tune virus replication  
578 and host response. *J Gen Virol* 96:756-66.
- 579 19. **Zheng M, Wang P, Song W, Lau SY, Liu S, Huang X, Mok BW, Liu  
580 YC, Chen Y, Yuen KY, Chen H.** 2015. An A14U Substitution in the 3'  
581 Noncoding Region of the M Segment of Viral RNA Supports  
582 Replication of Influenza Virus with an NS1 Deletion by Modulating  
583 Alternative Splicing of M Segment mRNAs. *J Virol* 89:10273-85.
- 584 20. **Ma J, Liu K, Xue C, Zhou J, Xu S, Ren Y, Zheng J, Cao Y.** 2013.  
585 Impact of the segment-specific region of the 3'-untranslated region of  
586 the influenza A virus PB1 segment on protein expression. *Virus Genes*  
587 47:429-38.
- 588 21. **Wang L, Lee CW.** 2009. Sequencing and mutational analysis of the  
589 non-coding regions of influenza A virus. *Vet Microbiol* 135:239-47.
- 590 22. **Maeda Y, Goto H, Horimoto T, Takada A, Kawaoka Y.** 2004.  
591 Biological significance of the U residue at the -3 position of the mRNA  
592 sequences of influenza A viral segments PB1 and NA. *Virus Res*  
593 100:153-7.
- 594 23. **Fujii K, Fujii Y, Noda T, Muramoto Y, Watanabe T, Takada A, Goto H,  
595 Horimoto T, Kawaoka Y.** 2005. Importance of both the coding and the  
596 segment-specific noncoding regions of the influenza A virus NS  
597 segment for its efficient incorporation into virions. *J Virol* 79:3766-74.
- 598 24. **Hutchinson EC, Curran MD, Read EK, Gog JR, Digard P.** 2008.  
599 Mutational analysis of cis-acting RNA signals in segment 7 of influenza  
600 A virus. *J Virol* 82:11869-79.
- 601 25. **Liang Y, Hong Y, Parslow TG.** 2005. cis-Acting packaging signals in  
602 the influenza virus PB1, PB2, and PA genomic RNA segments. *J Virol*  
603 79:10348-55.
- 604 26. **Marsh GA, Hatami R, Palese P.** 2007. Specific residues of the  
605 influenza A virus hemagglutinin viral RNA are important for efficient  
606 packaging into budding virions. *J Virol* 81:9727-36.
- 607 27. **Hutchinson EC, Wise HM, Kudryavtseva K, Curran MD, Digard P.**  
608 2009. Characterisation of influenza A viruses with mutations in segment  
609 5 packaging signals. *Vaccine* 27:6270-5.
- 610 28. **Gog JR, Afonso Edos S, Dalton RM, Leclercq I, Tiley L, Elton D,  
611 von Kirchbach JC, Naffakh N, Escriou N, Digard P.** 2007. Codon  
612 conservation in the influenza A virus genome defines RNA packaging  
613 signals. *Nucleic Acids Res* 35:1897-907.

- 614 29. **Fujii Y, Goto H, Watanabe T, Yoshida T, Kawaoka Y.** 2003. Selective  
615 incorporation of influenza virus RNA segments into virions. *Proc Natl*  
616 *Acad Sci U S A* 100:2002-7.
- 617 30. **Muramoto Y, Takada A, Fujii K, Noda T, Iwatsuki-Horimoto K,**  
618 **Watanabe S, Horimoto T, Kida H, Kawaoka Y.** 2006. Hierarchy  
619 among viral RNA (vRNA) segments in their role in vRNA incorporation  
620 into influenza A virions. *J Virol* 80:2318-25.
- 621 31. **Dos Santos Afonso E, Escriou N, Leclercq I, van der Werf S,**  
622 **Naffakh N.** 2005. The generation of recombinant influenza A viruses  
623 expressing a PB2 fusion protein requires the conservation of a  
624 packaging signal overlapping the coding and noncoding regions at the  
625 5' end of the PB2 segment. *Virology* 341:34-46.
- 626 32. **Watanabe T, Watanabe S, Noda T, Fujii Y, Kawaoka Y.** 2003.  
627 Exploitation of nucleic acid packaging signals to generate a novel  
628 influenza virus-based vector stably expressing two foreign genes. *J*  
629 *Virol* 77:10575-83.
- 630 33. **Marsh GA, Rabadan R, Levine AJ, Palese P.** 2008. Highly conserved  
631 regions of influenza A virus polymerase gene segments are critical for  
632 efficient viral RNA packaging. *J Virol* 82:2295-304.
- 633 34. **Ozawa M, Maeda J, Iwatsuki-Horimoto K, Watanabe S, Goto H,**  
634 **Horimoto T, Kawaoka Y.** 2009. Nucleotide sequence requirements at  
635 the 5' end of the influenza A virus M RNA segment for efficient virus  
636 replication. *J Virol* 83:3384-8.
- 637 35. **Liang Y, Huang T, Ly H, Parslow TG, Liang Y.** 2008. Mutational  
638 analyses of packaging signals in influenza virus PA, PB1, and PB2  
639 genomic RNA segments. *J Virol* 82:229-36.
- 640 36. **Odagiri T, Tashiro M.** 1997. Segment-specific noncoding sequences of  
641 the influenza virus genome RNA are involved in the specific  
642 competition between defective interfering RNA and its progenitor RNA  
643 segment at the virion assembly step. *J Virol* 71:2138-45.
- 644 37. **Wang J, Li J, Zhao L, Cao M, Deng T.** 2017. Dual Roles of the  
645 Hemagglutinin Segment-Specific Noncoding Nucleotides in the  
646 Extended Duplex Region of the Influenza A Virus RNA Promoter. *J Virol*  
647 91:e01931-16.
- 648 38. **Vreede FT, Jung TE, Brownlee GG.** 2004. Model suggesting that  
649 replication of influenza virus is regulated by stabilization of replicative  
650 intermediates. *J Virol* 78:9568-72.
- 651 39. **Widjaja I, de Vries E, Rottier PJ, de Haan CA.** 2012. Competition  
652 between influenza A virus genome segments. *PLoS One* 7:e47529.
- 653 40. **Hara K, Schmidt FI, Crow M, Brownlee GG.** 2006. Amino acid  
654 residues in the N-terminal region of the PA subunit of influenza A virus  
655 RNA polymerase play a critical role in protein stability, endonuclease  
656 activity, cap binding, and virion RNA promoter binding. *J Virol* 80:7789-  
657 98.



- 658 41. **Neverov AD, Kryazhimskiy S, Plotkin JB, Bazykin GA.** 2015.  
659 Coordinated Evolution of Influenza A Surface Proteins. *PLoS Genet*  
660 11:e1005404.
- 661 42. **Gaymard A, Le Briand N, Frobert E, Lina B, Escuret V.** 2016.  
662 Functional balance between neuraminidase and haemagglutinin in  
663 influenza viruses. *Clin Microbiol Infect* 22:975-983.
- 664 43. **Diederich S, Berhane Y, Embury-Hyatt C, Hisanaga T, Handel K,**  
665 **Cottam-Birt C, Ranadheera C, Kobasa D, Pasick J.** 2015.  
666 Hemagglutinin-Neuraminidase Balance Influences the Virulence  
667 Phenotype of a Recombinant H5N3 Influenza A Virus Possessing a  
668 Polybasic HA0 Cleavage Site. *J Virol* 89:10724-34.
- 669 44. **Xu R, Zhu X, McBride R, Nycholat CM, Yu W, Paulson JC, Wilson**  
670 **IA.** 2012. Functional balance of the hemagglutinin and neuraminidase  
671 activities accompanies the emergence of the 2009 H1N1 influenza  
672 pandemic. *J Virol* 86:9221-32.
- 673 45. **Yen HL, Liang CH, Wu CY, Forrest HL, Ferguson A, Choy KT,**  
674 **Jones J, Wong DD, Cheung PP, Hsu CH, Li OT, Yuen KM, Chan**  
675 **RW, Poon LL, Chan MC, Nicholls JM, Krauss S, Wong CH, Guan Y,**  
676 **Webster RG, Webby RJ, Peiris M.** 2011. Hemagglutinin-  
677 neuraminidase balance confers respiratory-droplet transmissibility of  
678 the pandemic H1N1 influenza virus in ferrets. *Proc Natl Acad Sci U S A*  
679 108:14264-9.
- 680 46. **Dadonaite B, Gilbertson B, Knight ML, Trifkovic S, Rockman S,**  
681 **Laederach A, Brown LE, Fodor E, Bauer DLV.** 2019. The structure of  
682 the influenza A virus genome. *Nat Microbiol* 4:1781-1789.
- 683 47. **Le Sage V, Kanarek JP, Snyder DJ, Cooper VS, Lakdawala SS, Lee**  
684 **N.** 2020. Mapping of Influenza Virus RNA-RNA Interactions Reveals a  
685 Flexible Network. *Cell Rep* 31:107823.
- 686 48. **Fodor E, Crow M, Mingay LJ, Deng T, Sharps J, Fechter P,**  
687 **Brownlee GG.** 2002. A single amino acid mutation in the PA subunit of  
688 the influenza virus RNA polymerase inhibits endonucleolytic cleavage  
689 of capped RNAs. *J Virol* 76:8989-9001.
- 690 49. **Hoffmann E, Neumann G, Kawaoka Y, Hobom G, Webster RG.**  
691 2000. A DNA transfection system for generation of influenza A virus  
692 from eight plasmids. *Proc Natl Acad Sci U S A* 97:6108-13.
- 693 50. **Tannock GA, Paul JA, Barry RD.** 1984. Relative immunogenicity of  
694 the cold-adapted influenza virus A/Ann Arbor/6/60 (A/AA/6/60-ca),  
695 recombinants of A/AA/6/60-ca, and parental strains with similar surface  
696 antigens. *Infect Immun* 43:457-62.
- 697 51. **Robb NC, Smith M, Vreede FT, Fodor E.** 2009. NS2/NEP protein  
698 regulates transcription and replication of the influenza virus RNA  
699 genome. *J Gen Virol* 90:1398-407.
- 700 52. **Schneider CA, Rasband WS, Eliceiri KW.** 2012. NIH Image to  
701 ImageJ: 25 years of image analysis. *Nat Methods* 9:671-5.

## FIGURE LEGENDS

**FIG 1** The 3'-end H1-ssNCR is not essential for transcription and replication in single-template vRNP reconstitution assays. (A) Schematic representation of mutants with serial truncations at the 3'-end H1-ssNCR of the HA segment of WSN virus. The red boxes represent the 3' and 5' terminal promoter regions. The orange boxes represent the start codon (AUG) of HA vRNA (UAC in negative sense). The lines represent the remaining nucleotides. The triangles represent the deleted nucleotides. The truncation is three nucleotides at a time. In 3L6, the short line next to the red box at the 3' end represents two conserved nucleotides CC (in negative sense) next to the 3' terminal promoter region. (B, C) HEK-293T cells were cotransfected with plasmids expressing WSN (B) or CA04 (C) viral polymerase subunits, NP and wildtype or mutant HA vRNA (wildtype or mutant). A polymerase containing an active site mutation (PB1a: D445A/446A) was used as negative control (NC). Accumulation of RNA 24h post-transfection was analysed by primer extension and 6% PAGE. SE: short exposure; LE: long exposure. The graph shows the mean intensity signals of mutant HA RNAs relative to those of wildtype HA RNAs. The data represent the means  $\pm$  standard error of mean (s.e.m) of three independent experiments.

**FIG 2** Truncations of the 3'-end H1-ssNCR lead to reduced virus replication. (A, B) Titres of WSN (A) and CA04 (B) rescued viruses (P0). Wildtype or mutant viruses were rescued in HEK-293T cells by cotransfecting eight pHW2000-PB2, -PB1, -PA, -HA (wildtype or mutant), -NP, -NA, -M and -NS plasmids. The graph shows the mean titres of wildtype and mutant viruses. The data represent the means  $\pm$  s.e.m of three independent experiments. One-way analysis of variance (ANOVA) with Dunnett correction for multiple testing; asterisks represent a significant difference from wildtype virus as follows:  $P < 0.01$  (\*\*),  $P < 0.001$  (\*\*\*),  $P < 0.0001$  (\*\*\*\*). (C) Growth curves of WSN viruses. The growth curves of the WSN viruses were determined by plaque assay on MDCK cells at 24 h, 36 h, 48 h, 60 h and 72 h post-infection. The graph shows the mean titres of wildtype and mutant viruses. The data represent the means  $\pm$  s.e.m of three independent experiments. Two-way analysis of variance (ANOVA) with Dunnett correction for multiple testing; asterisks represent a significant difference from wildtype virus as follows:  $P < 0.05$  (\*),  $P < 0.01$  (\*\*). (D) Titres of CA04 wildtype and mutant viruses (P6). CA04 WT, 3L5 and 3L6 were passaged in embryonated eggs for six times (P6) and the P6 virus titres were detected by TCID<sub>50</sub>. The data represent the means  $\pm$  s.e.m of three independent experiments. One-way analysis of variance (ANOVA) with Dunnett correction for multiple testing; asterisks represent a significant difference from wildtype virus as follows:  $P < 0.01$  (\*\*),  $P < 0.001$  (\*\*\*). (E, F) Reverse complementary DNA sequences of the 3'

terminus of WSN (E) or CA04 (F) HA vRNA of viruses harvested at 48 h post-infection from the growth curve experiment above. The sequencing results are the representatives from three independent biological replicates (n=3).

**FIG 3** The G76A and C56U mutations improve the growth of 3L4 and 3L5 viruses. (A) Titres of rescued viruses (P0). Wildtype or mutant viruses were rescued in HEK-293T cells and virus titres were examined by plaque assay on MDCK cells. The graph shows the mean titres of wildtype and mutant viruses. The data represent the means  $\pm$  s.e.m of three independent experiments. Two-way analysis of variance (ANOVA) with Dunnett correction for multiple testing; asterisks represent a significant difference from wildtype virus as follows:  $P<0.0001$ (\*\*\*\*). (B) Reverse complementary DNA sequence traces of the 3' terminus HA vRNA of 3L4, 3L4-G76A, 3L5 and 3L5-G76A mutant viruses from panel (A). The sequence traces are the representatives from three independent biological replicates (n=3). (C) Titres of WSN wildtype and mutant viruses (P2). WSN WT, 3L5-G76A and 3L5-C56U were passaged in MDCK cells twice (P2) and the P2 virus titres were detected by plaque assay.

**FIG 4** The 3'-end H1-ssNCR truncated mutant viruses show decreased HA vRNA levels in virions and in cells. (A, B) Wildtype or mutant viruses were rescued in HEK-293T cells and then passaged in MDCK cells once. The vRNA levels of P0(A) and P1(B) virus in virions and in cells were analysed by RT-qPCR. The graphs show the mean values of HA vRNA relative to those of NA vRNA. The data represent the means  $\pm$  s.e.m of three independent experiments. Two-way analysis of variance (ANOVA) with Dunnett correction for multiple testing; asterisks represent a significant difference from wildtype virus as follows:  $P<0.05$  (\*),  $P<0.01$ (\*\*),  $P<0.001$ (\*\*\*),  $P<0.0001$ (\*\*\*\*).

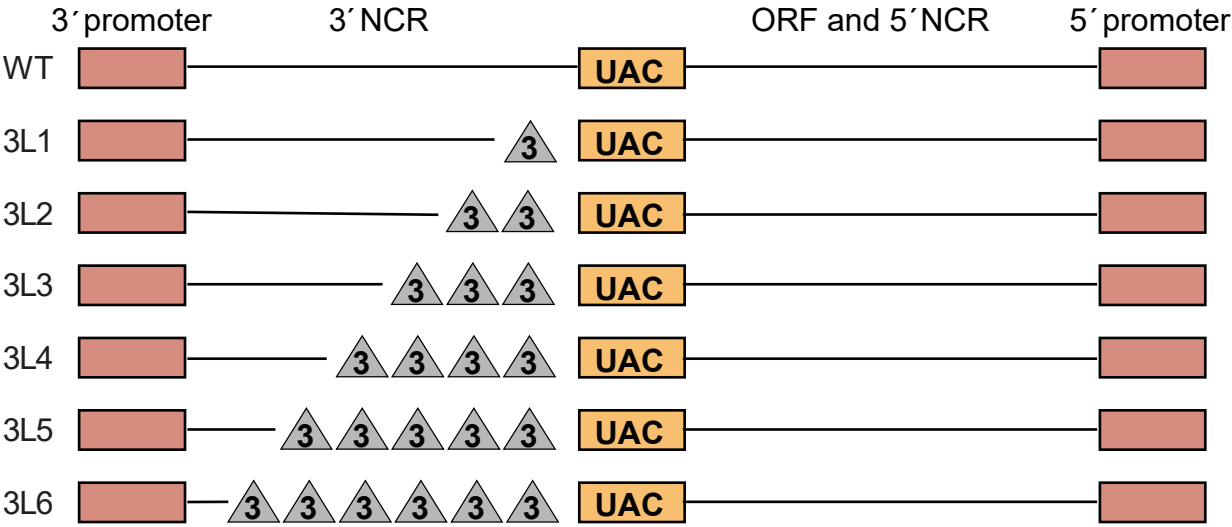
**FIG 5** The 3'-end H1-ssNCR truncated mutant templates are replicated less efficiently than the wildtype HA template in multiple-template vRNP reconstitution assays. (A, B) Seven pHW2000-PB2, -PB1, -PA, -HA (wildtype or mutant), -NP, -NA and -NS plasmids derived from WSN (A) or CA04 (B) were transfected into HEK-293T cells. A polymerase containing an active site mutation (PB1a: D445A/446A) was used as negative control (NC). Accumulation of HA and NA RNAs was analysed by primer extension and 6% PAGE. The graph shows the mean intensity signals of mutant HA and NA RNAs relative to those of wildtype RNAs. The data represent the means  $\pm$  s.e.m of three independent experiments. Two-way analysis of variance (ANOVA) with Dunnett correction for multiple testing; asterisks represent a significant difference from wildtype virus as follows:  $P<0.05$  (\*),  $P<0.01$ (\*\*),  $P<0.001$ (\*\*\*),  $P<0.0001$ (\*\*\*\*).

**FIG 6** The G76A and C56U mutations increased the replication of the 3'-terminal H1-ssNCR truncated mutant template in multi-template vRNP recombination assays. HEK-293T cells were cotransfected with pcDNA-PB2, pcDNA-PB1, pcDNA-PA-D108A, pcDNA-NP, pPOL1-HA and pPOL1-mut-HA

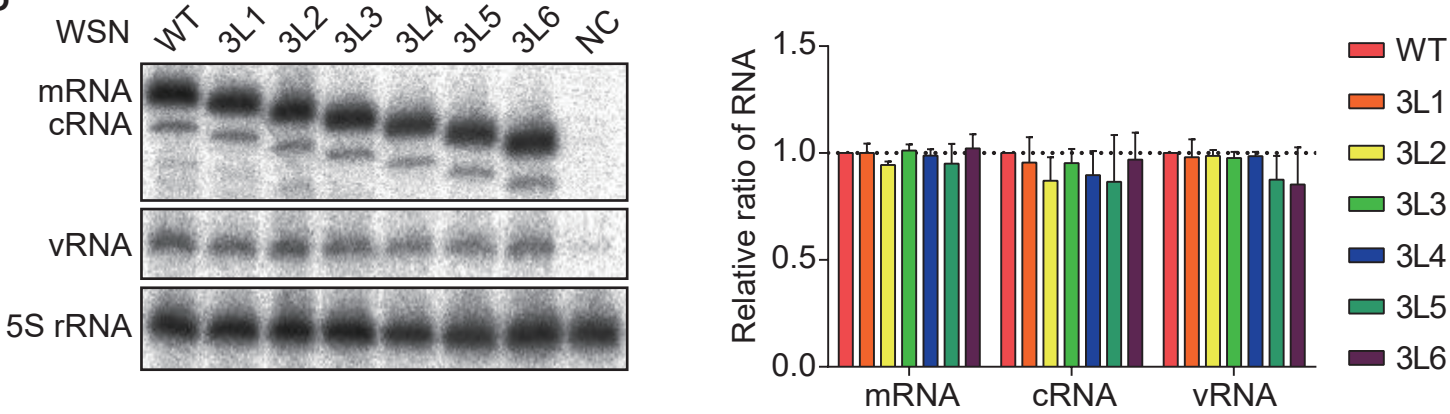
786 with G76A(A) or C56U(B). A polymerase containing an active site mutation  
787 (PB1a: D445A/446A) was used as negative control (NC). Accumulation of  
788 RNA 24h post-transfection was analysed by primer extension. The graph  
789 shows the mean intensity signals of mutant HA RNAs relative to those of  
790 wildtype HA RNAs. The data represent the means  $\pm$  s.e.m of three  
791 independent experiments. Two-way analysis of variance (ANOVA) with  
792 Dunnett correction for multiple testing; asterisks represent a significant  
793 difference from wildtype virus as follows:  $P < 0.05$  (\*),  $P < 0.01$  (\*\*),  $P < 0.001$  (\*\*\*),  
794  $P < 0.0001$  (\*\*\*\*).

FIGURE 1

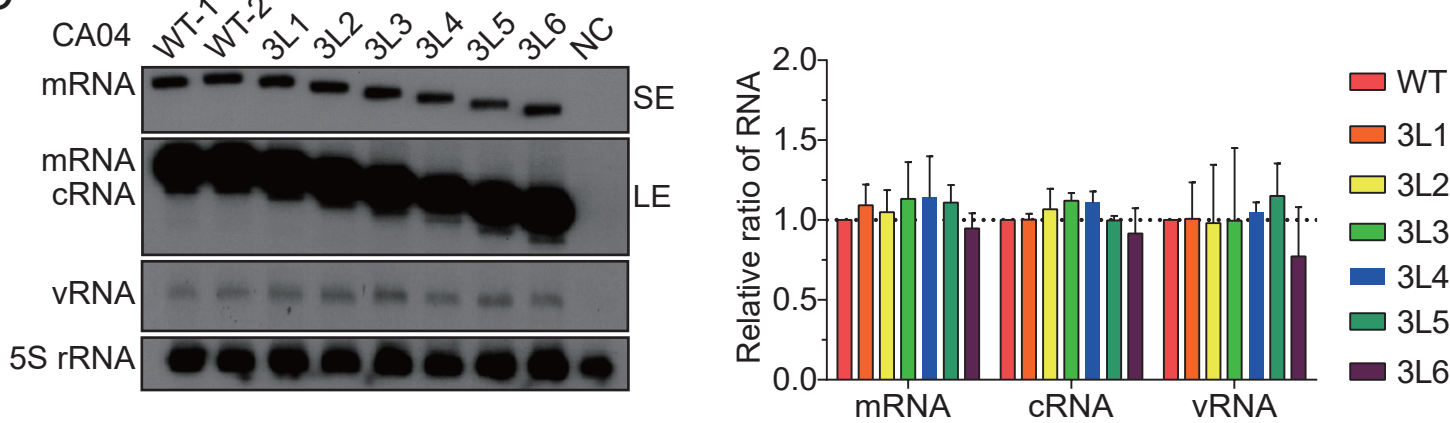
A



B



C



**A** WSN viruses rescued in 293T cells (P0)

Strain	Virus titre (log <sub>10</sub> PFU/ml)
WT	~6.5
3L1	~6.6
3L2	~6.1
3L3	~5.5 (**)
3L4	~3.1 (****)
3L5	~3.0 (****)
3L6	Non-detectable

**B** CA04 viruses rescued in 293T cells (P0)

Strain	Virus titre (Log <sub>10</sub> TCID <sub>50</sub> /ml)
WT	~5.0
3L1	~4.7
3L2	~4.6
3L3	~4.6
3L4	~4.0 (***)
3L5	~3.0 (****)
3L6	~2.7 (****)

**C** WSN viruses passaged in MDCK cells (P2)

Time post-infection (h)	WT	3L1	3L2	3L3	3L4	3L5
24	~6.0	~5.5	~5.2	~5.0	~5.0	~5.0
36	~8.0	~7.8	~7.5	~7.5	~7.5	~7.5
48	~8.5	~8.2	~7.8	~7.8	~7.8	~7.8
60	~8.0	~7.8	~7.5	~7.5	~7.5	~7.5
72	~7.8	~7.5	~7.2	~7.2	~7.2	~7.2

**D** CA04 viruses passaged in eggs (P6)

Strain	Virus titre (Log <sub>10</sub> TCID <sub>50</sub> /ml)
WT	~6.2
3L5	~4.3 (***)
3L6	~5.3 (**)

**E** WSN viruses

**F** CA04 viruses

FIGURE 3

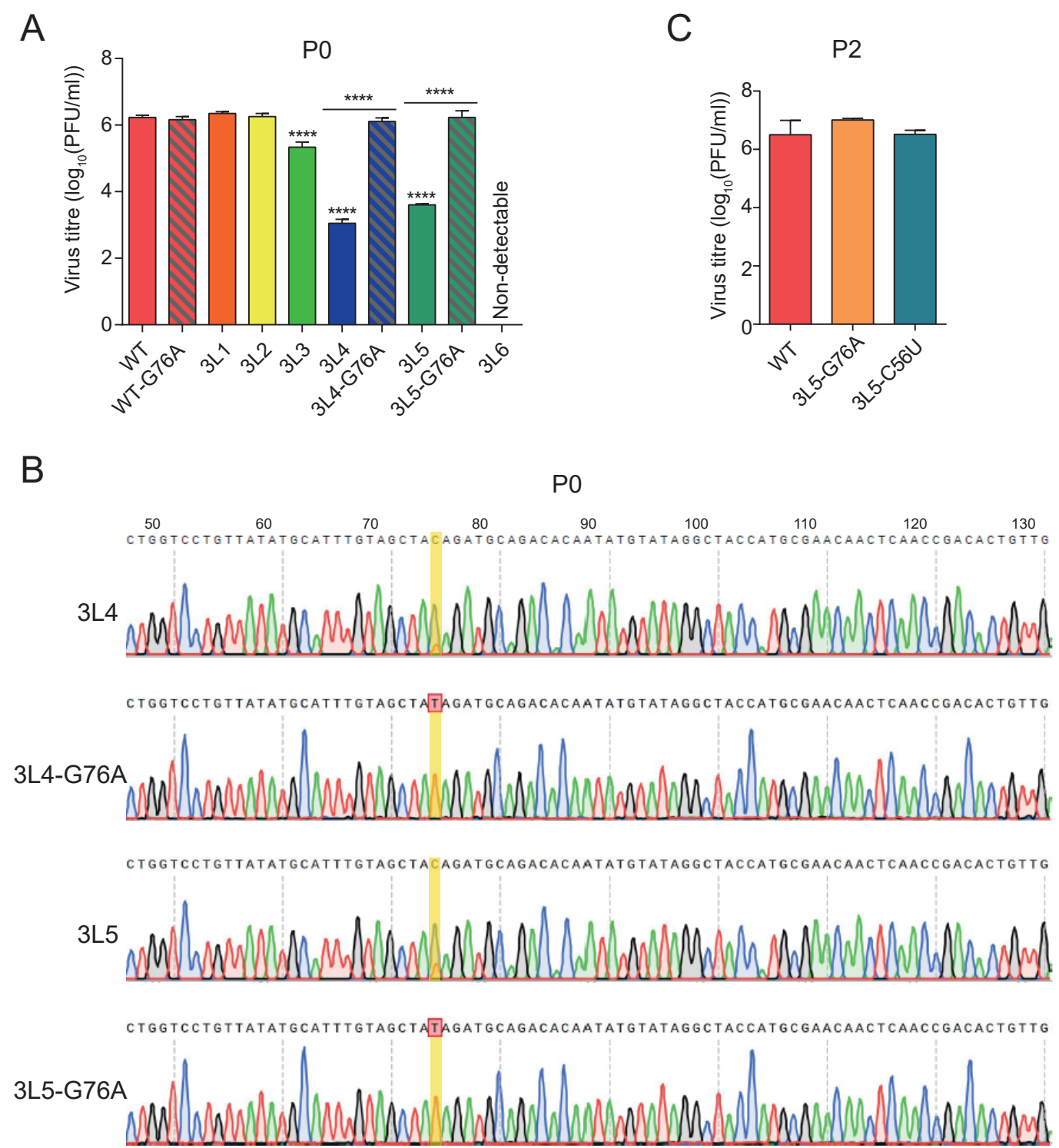


FIGURE 4

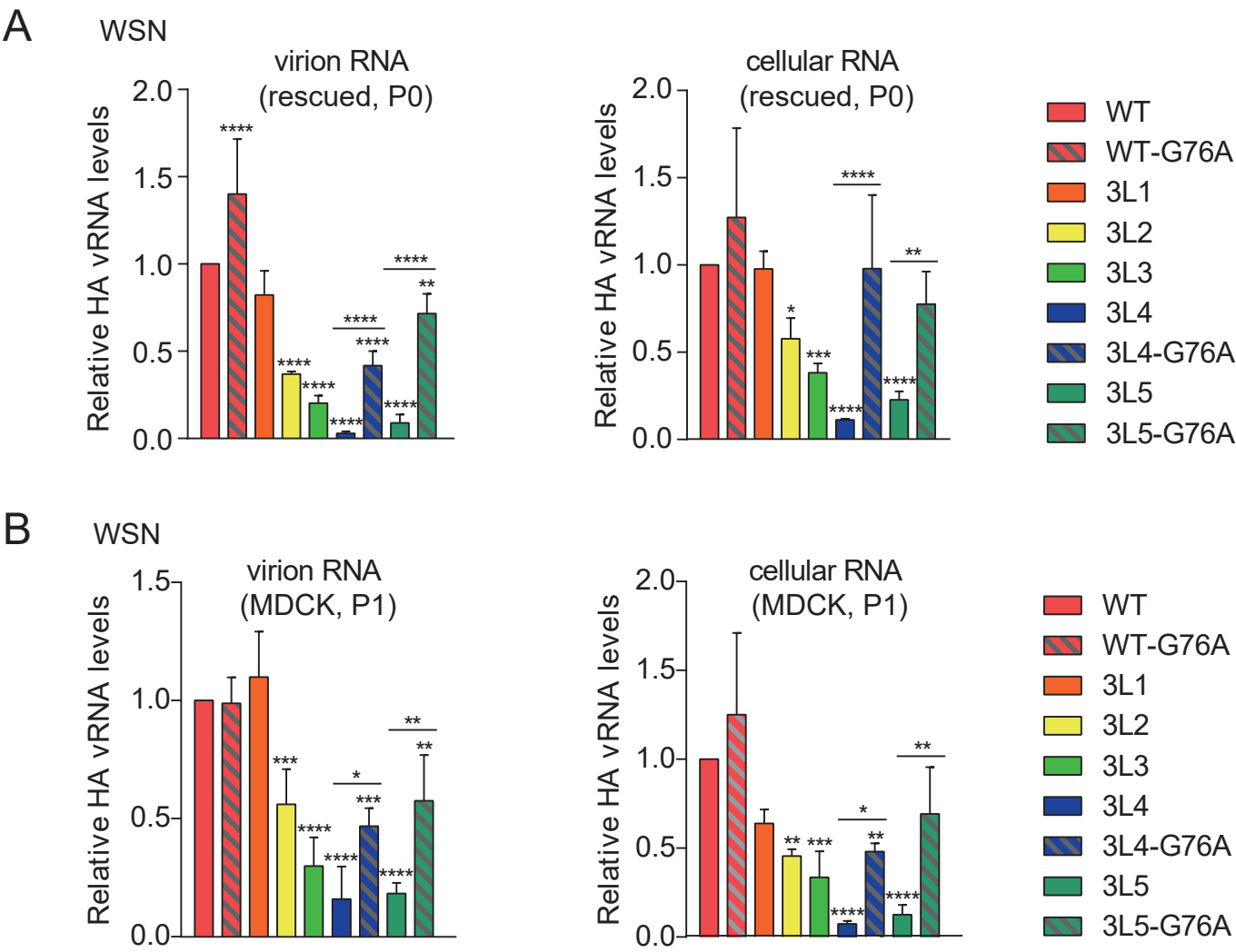




FIGURE 5

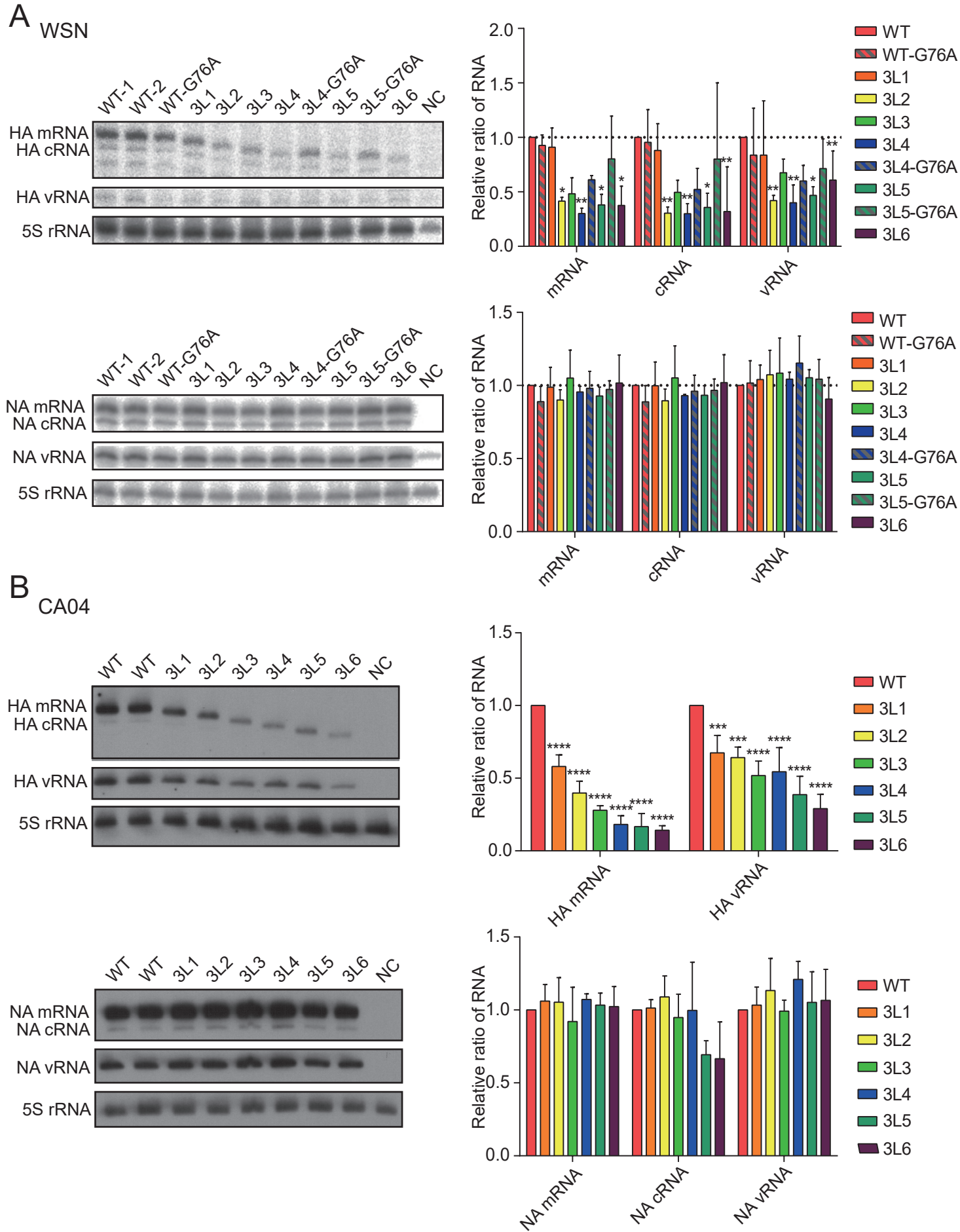


FIGURE 6

